

# NJC

Accepted Manuscript



This is an *Accepted Manuscript*, which has been through the Royal Society of Chemistry peer review process and has been accepted for publication.

*Accepted Manuscripts* are published online shortly after acceptance, before technical editing, formatting and proof reading. Using this free service, authors can make their results available to the community, in citable form, before we publish the edited article. We will replace this *Accepted Manuscript* with the edited and formatted *Advance Article* as soon as it is available.

You can find more information about *Accepted Manuscripts* in the [Information for Authors](#).

Please note that technical editing may introduce minor changes to the text and/or graphics, which may alter content. The journal's standard [Terms & Conditions](#) and the [Ethical guidelines](#) still apply. In no event shall the Royal Society of Chemistry be held responsible for any errors or omissions in this *Accepted Manuscript* or any consequences arising from the use of any information it contains.



[www.rsc.org/njc](http://www.rsc.org/njc)

## ARTICLE

# Piperazine derivatives of boronic acids - potential bifunctional biologically active compounds

Cite this: DOI: 10.1039/x0xx00000x

Agnieszka Adamczyk-Woźniak\*<sup>a</sup>, Karolina Czerwińska<sup>a</sup>, Izabela D. Madura<sup>a</sup>, Alicja Matuszewska<sup>a</sup>, Andrzej Sporzyński<sup>a</sup> and Anna Żubrowska-Zembruska<sup>a</sup>

Received 00th January 2015,

Accepted 00th January 2015

DOI: 10.1039/x0xx00000x

www.rsc.org/

The combination of a piperazine and boronic groups within one molecule can result in totally novel biological activity. Series of benzyl piperazine derivatives of boronic acids have been obtained by the facile and effective method based on amination-reduction reaction of 2-formylphenylboronic acids with *N*-substituted piperazines. Molecular and crystal structures of six novel derivatives have been investigated with support of Hirshfeld surface analysis and hydrogen bond energy estimation. The studied compounds display several structural features that make them promising candidates for biologically active compounds.

## Introduction

The piperazine scaffold is frequently found in biologically active compounds probably due to their affinity to various receptors.<sup>1-3</sup> Many phenyl and benzyl piperazine derivatives are notable successful drugs, including: antianginals (e.g. Trimetazidine),<sup>4</sup> antidepressants (e.g. Trazodone),<sup>5</sup> antihistamines (e.g. Cyclizine and Cetirizine,<sup>6</sup> Buclizine,<sup>7</sup> Cinnarizine<sup>8</sup>) as well as antipsychotics (e.g. Aripiprazole).<sup>9</sup> Some other arylpiperazines are currently at the clinical trials.<sup>10</sup> There are also many so-called recreational drugs of the piperazine structure e.g. 1-benzylpiperazine (BZP),<sup>11</sup> 4-methyl-1-benzylpiperazine (MBZP), 4-fluorophenylpiperazine (pFPP) and 2,3-dichlorophenylpiperazine (DCPP), some of them becoming illegal.<sup>12</sup> Further, Imatinib - the piperazine containing potent anticancer drug - is the first one that acts specifically by inhibiting a certain enzyme rather than by killing all the rapidly dividing cells.<sup>13</sup> Similar action displays the recently developed boronic anticancer drug called Bortezomib, inhibiting the Proteasome 26S receptor<sup>14</sup> (Figure 1). It should be noted that the boronic acid moiety, able to reversibly form complexes with hydroxyl compounds, can be responsible for binding to a specific bio-molecule.<sup>15,16</sup> Therefore, the combination of a piperazine and boronic groups within one molecule can result in totally novel biological activity (Figure 2). What is more, the proximity of the nitrogen atom usually increases the affinity of the boronic acid towards hydroxyl compounds, enabling their binding at physiological pH.<sup>17</sup> The structure of the amine substituent can also influence the selectivity of the complexation.<sup>18</sup> Additionally, the ester formation with cis-diols can considerably change physicochemical properties of the molecule, e.g. its solubility in lipids, altering the crossing of the

blood-brain barrier. The esterification of the boronic unit enables also alternative drug formulation as in the case of Bortezomib, which is actually used as its mannitol ester.<sup>19</sup> The considered compounds can also act as useful building-blocks, the Suzuki coupling of which should result in novel biphenyl piperazine derivatives,<sup>20</sup> which display the acetylcholine receptor antagonists' activity<sup>21</sup> as well as selective, and reversible inhibition of Cathepsin K enzyme.<sup>22</sup>

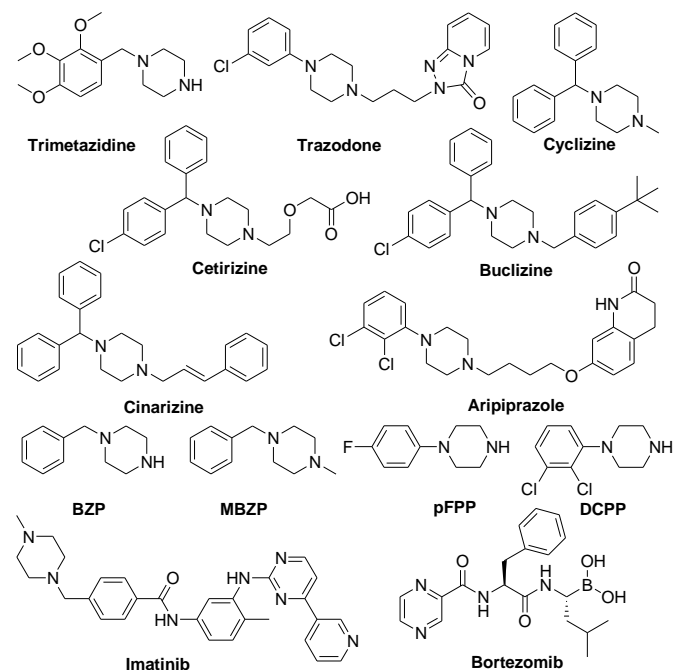


**Figure 1.** Some of the benzyl or phenylpiperazine drugs and Bortezomib.

The investigation of potential biologically active compounds/drugs very often starts from the design based on the crystal structure analysis.<sup>23,24</sup> The detailed structural studies can point out for example the stable conformations<sup>25</sup> or preferred intermolecular interactions,<sup>26</sup> the parameters being important for molecular recognition or binding with protein active sites.<sup>16,27</sup> Therefore, we have undertaken studies on selected new piperazine-boronic acid bifunctional molecules (Figure 2). Both the facile and effective synthetic method and valuable information coming from crystal structure investigations supported by Hirshfeld surface analysis,<sup>28</sup> and hydrogen bond energy estimation<sup>29</sup> are presented.

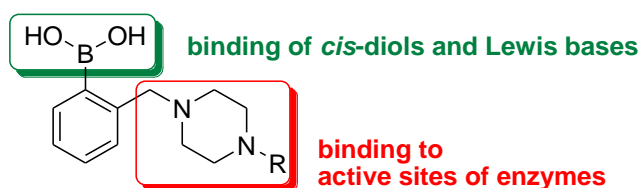


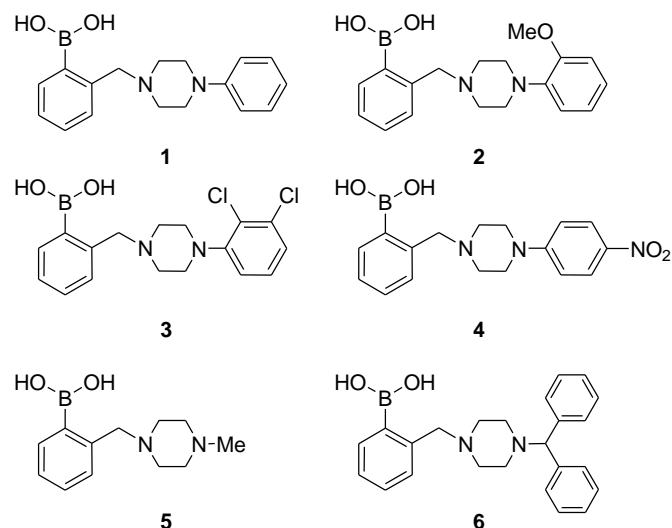
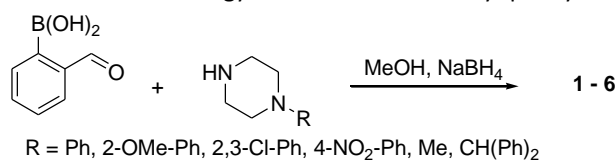
**Figure 2.** Proposed mode of action of studied novel bifunctional piperazine derivatives of boronic acids.

## Result and discussion

### General remarks

Despite the potential importance of the molecules combining piperazine as well as boronic scaffolds (Figure 2), only few boronic derivatives of piperazines have been obtained and studied so far.<sup>30,31</sup> These, which were structurally characterized are the *ortho* CH<sub>2</sub>-piperazine substituted bisboronic acids and hemiesters, including benzoxaboroles,<sup>31</sup> as well as monoboronic acid pinacole esters.<sup>30</sup> In all of them no N→B dative bond was observed what was attributed to the lack of the activity against thrombin.<sup>30a</sup> However, the boronic acid esters do not form strong hydrogen bonds,<sup>32</sup> while H-bonds were found to be competing with the dative bond in case of *ortho* substituted boronic acids.<sup>33</sup> What is more, the role of a hydrogen bond donor group for the affinity and selectivity towards the α<sub>1</sub>B-adrenoceptors, postulated by Bremner's pharmacophore model<sup>1a</sup> was confirmed by functional and molecular modeling studies.<sup>2</sup> There is also evidence given by protein crystallography that boronic acids are H-bonded active species during binding processes.<sup>16,34</sup> Therefore, we decided to synthesize and study *ortho* substituted phenylboronic monoacids with selected piperazines, including analogues of already known drugs (Scheme 1). Compounds **1** and **5** can be treated as model ones to show the differences introduced by aromatic (**1-4**) or aliphatic (**5-6**) substituent in the piperazine scaffold on molecular geometry,<sup>35</sup> as well as types of possible intermolecular interactions. Additionally, the relatively long substituents in **4** and **6** were chosen to study the role of spatial

requirements in molecular packing. Compounds **1-6** have been obtained according to the recently optimized amination-reduction methodology for the 2-aminomethyl phenylboronic



acids (Scheme 1).<sup>36</sup>

**Scheme 1.** Synthetic strategy for benzyl piperazine derivatives of phenylboronic acids.

### Crystal structures

The products were recrystallized to give the crystals suitable for single crystal X-ray diffraction experiments. The results confirmed pure crystals of **1**, **3**, **4** and solvates of **5**, **6**. In the case of **2** the high residual electron density was observed during structure refinement indicating the presence of a severely disordered or diffused solvent (see Supporting information).

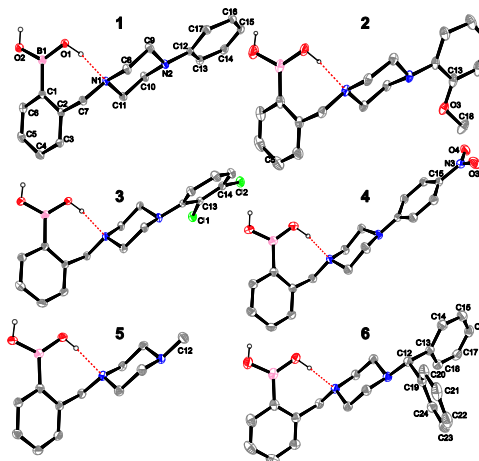


**Figure 3.** Ortep drawing<sup>37</sup> with atoms numbering scheme of studied molecules. The ellipsoids are shown at 50% probability.

The intramolecular O–H...N hydrogen bonds are denoted with dashed lines. Only hydrogen atoms of hydroxyl groups are given. In case of **6** only the molecule A is presented.

The studied molecules crystallize in centrosymmetric space groups except for molecules of **5** that crystallize in non-centrosymmetric  $Pna2_1$  space group of the orthorhombic system (Table 2). In the case of **6** there are two crystallographically independent molecules in the asymmetric part of the unit cell. The minor differences between these two molecules in torsion angles were detected only (Table S1). Generally, the geometry of all investigated molecules is akin (Table S1). Boron atom shows trigonal coordination while OH groups adopt *syn-anti* conformation (Figure 3). The B(OH)<sub>2</sub> moiety is substantially twisted with respect to the phenyl ring and the twist angle varies from 16.76(5)<sup>o</sup> for **1** to 26.68(1)<sup>o</sup> in **5** (Table S1).

**Table 1.** Geometrical parameters of the H-bonds in crystals of **1-6**. The bonds are given in Å, angles in<sup>o</sup>. The estimated energy is given in kcal/mol.

Compound	H...A	D...A	D–H...A	Energy
<b>1</b>				
O1–H1...N1	1.77(2)	2.666(1)	167(2)	6.1
O2–H2...O1 <sup>[a]</sup>	1.89(2)	2.756(1)	177(2)	3.3
<b>2</b>				
O1–H1...N1	1.78	2.614(2)	170	8.2
O2–H2...O1 <sup>ii</sup>	1.94	2.768(2)	168	2.9
<b>3</b>				
O1–H1...N1	1.79(3)	2.615(2)	164(3)	7.3
O2–H2...O1 <sup>iii</sup>	2.03(3)	2.824(2)	170(3)	2.2
<b>4</b>				
O1–H1...N1	1.75(2)	2.659(1)	168(2)	6.4
O2–H2...O3 <sup>iv</sup>	2.11(2)	2.9465(13)	165(2)	1.1
<b>5</b>				
O1–H1...N1	1.85	2.682(2)	169	5.8
O2–H2...N2 <sup>v</sup>	1.95	2.712(2)	150	3.0
O3–H3B...O2 <sup>vi</sup>	1.98	2.802(2)	163	2.2
O3–H3A...O1 <sup>vii</sup>	2.05	2.887(2)	167	1.5
<b>6</b>				
O1–H1...N1	1.75	2.587(1)	173	9.8
O3–H3...N3	1.81	2.633(1)	168	7.2
O2–H2...O3	1.90	2.7426(13)	175	3.5
O3–H4...O1	1.86	2.696(1)	174	4.5

[a] Symmetry codes: (i) 1-x,1-y,1-z; (ii) 1/2-x,1/2-y,3/2-z; (iii) -x,-y,1-z; (iv) -1/2+x,1/2-y,-1/2+z; (v) 1/2-x,1/2+y,-1/2+z; (vi) 1/2-x,-1/2+y,1/2+z; (vii) 1-x,1-y,1/2+z.

As recently shown,<sup>38</sup> the differences in this parameter may result from intermolecular interactions, but the intra- ones should be also taken into account.<sup>39</sup> Further, in all the cases the piperazine fragment adopts a chair conformation with comparable geometrical parameters except for the pyramidalization of N2 atom (Table S1). It results from the

different nature of the piperazine substituents. In the case of compounds **1-4** the aromatic fragment tends to conjugate with the nitrogen atom causing the decrease of both the pyramidalization as well as N2–C12 bond length (Table S1). For compound **5** and **6** the N2 bond with aliphatic C12 carbon atom is by ~0.06 Å longer while the N2 atom deviates from plane defined by the three bonded atoms by more than 0.5 Å.

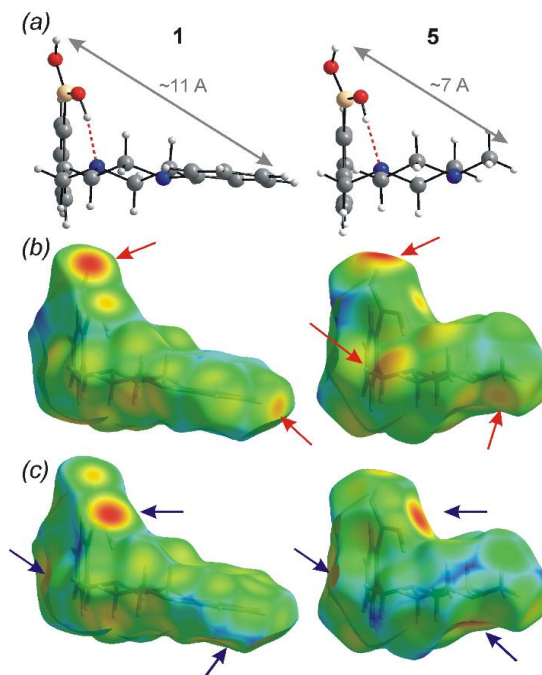


**Figure 4.** Side view of model molecules of **1** and **5** (a). Hirshfeld surfaces for **1** and **5** in form of  $d_f$  (b) and  $d_b$  (c). Red and blue arrows indicate donors and acceptors in intermolecular hydrogen bonds, respectively.

In the whole analyzed series the formation of intramolecular O1–H1...N1 hydrogen bond with  $S(7)$  graph designator<sup>40</sup> was detected. The values of O...N distance range from 2.587(1) to 2.682(2) Å while the O–H...N angle oscillates around 170<sup>o</sup> (Table 1). These values suits perfectly to these found for the whole range of  $S(7)$  rings in the case of variously *ortho*-substituted phenylboronic acids.<sup>39</sup> To better compare the resulting interactions, an energy estimation based on Lippincott and Schroeder one-dimensional H-bond model was performed.<sup>29</sup> The values range from 6 to 10 kcal/mol that places these interactions among strong hydrogen bonds.<sup>41</sup> Therefore, it can be assumed that this O1–H1...N1 hydrogen bond induces the *syn-anti* conformation of the boronic moiety. However, the difference in the nature of piperazine substituent seems not likely to influence this intramolecular H-bond (Table 1) as both the weakest and the strongest H-bonds are found in aliphatic analogues. What is more, the difference in the H-bond energy in molecules A and B of **6** being over 2.5 kcal/mol may suggest that the intermolecular interactions are decisive for the twist and simultaneously influence the intramolecular hydrogen bond strength. Nevertheless, the formation of strong

intramolecular H-bond causes that these boronic acid derivatives may further assemble *via* one strong hydrogen bond donor only, similarly as in the usually more active benzoxaborole derivatives.<sup>31,42</sup>

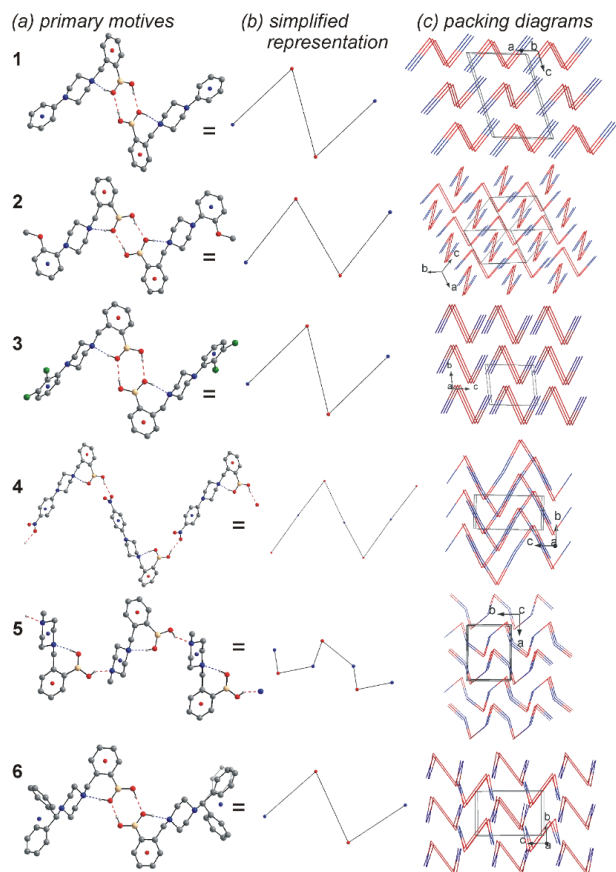


**Figure 5.** (a) Primary motives with their mutual arrangement. The hydrogen bonds are given with dash lines; (b) simplified model of the primary motif derived by connection (in line with H-bonds) of nodes (center of gravity of phenyl rings). Red and blue colours of nodes represent the boronic and piperazine fragments, respectively. (c) Packing diagrams of primary motives in simplified representations (see Fig. S2 in Electronic Supplementary Information for full packing diagrams). The solvent molecules in **5** and **6** are omitted.

To investigate the most probable interacting sites of the studied potentially active compounds, derivatives **1** and **5** were chosen as model ones. Figure 4a presents the overall shape of these molecules in crystals. The boronic and piperazine fragments locate almost perpendicularly, with the distance between foremost fragments being around 11 and 6 Å in case of **1** and **5**, respectively. The calculated molecular Hirshfeld surfaces (HS) with mapped  $d_i$  and  $d_e$  properties are presented in Figures 4b and 4c. They reflect the donor and acceptor properties of the molecules in terms of intermolecular interactions in crystal, respectively. It is noteworthy that such surfaces can also serve as starting points to model interactions with proteins.<sup>26,27</sup> It was also recently found, that the benzylpiperazine scaffold can dock either via hydrogen bonds or edge-to-face interactions.<sup>43</sup> In turn, the phenylboronic fragment may interact via hydrogen

bonds, aromatic or electron donor-acceptor interactions.<sup>16</sup> The mapped  $d_i$  on the HS surface suggests that the best H-bond donors are the *syn* oriented OH group and CH groups of the phenyl ring from boronic fragment. Additionally, in **1**, the phenyl substituent of piperazine fragment serves as a donor site in weak hydrogen bonds, while the lack of the aromatic counterpart in the case of **5** causes the activation of CH donors of the piperazine ring (Table S2). Both the oxygen atoms and aromatic ring/rings can act as the H-bond acceptors (Figure 4c, Table S2). Noteworthy are the enhanced acceptor properties of N2 atom in case of **5** resulting from its better availability (i.e. small, not conjugating substituent) comparing to other studied compounds.

The dual role of boronic OH group in hydrogen bonds is observed in the case of **1**, **2**, **3** and **6** where the O–H...O hydrogen bonded dimers are formed (Figure 5a). The estimated energy of these interactions is substantially lower than that of intramolecular O–H...N bonds and range from 2.2 to 4.5 kcal/mol (Table 1). In **4**, the O–H...O hydrogen bond is also formed, but in this case the NO<sub>2</sub> group acts as the acceptor. The resulting chain motif can be described with C(16) graph.<sup>40</sup> This H-bond is nearly twice weaker than these leading to dimeric motives and amounts to 1 kcal/mol only. The different arrangement in **4** might result from steric factors, i.e. long piperazine fragment. Nevertheless, the packing index<sup>44</sup> of all the studied molecules is relatively high and exciding 70% of the crystal lattice despite the form of the O–H...O bonded primary motives (Figure 5a).

Noteworthy is the different packing of dimers in the case of **2** (Figure 5c). The residual electron density was found at the final step of the structure refinement but the attempts to ascribe it to any solvent molecule/molecules were not successful. The diffusion of the solvent cannot be excluded what might explain the differences in packing of dimers in **2**. The solvent molecules were found in both aliphatic derivatives. In **5** it is a water molecule while in **6** two independent molecules of acetone were distinguished. In this case a minor influence of the acetone molecules on packing of dimers in **6** is observed comparing to structures of **1** and **3** (Figure 5c). On the contrary, the water molecule is strongly interacting with **5** serving as a hydrogen bond donor, thus competing with boronic hydroxyl groups. The observed intermolecular interactions are far different here than in the other studied analogues. First of all, the N2 atom is engaged in the hydrogen bond with boronic moiety and this interaction is of similar strength as these found for dimers. The C(10) chain motif is formed joining the molecules of **5** while the water molecule serves as linkers through the O–H...O bonds with boronic moiety, acting as a H-bond acceptor. The energy of these interchain H-bonds is substantially lower than in the main O–H...N chain (Table 1). This may suggest that the found active binding sites of this molecule might be effective in interactions with biomolecules even though water molecules are present.

## Conclusions

We have synthesized and structurally characterized six novel bifunctional compounds composed of phenylboronic acid fragment and selected piperazine derivatives with promising features to enhance their binding properties. The molecules were found not to be affected by piperazine N2 substituents except the N2–C12 bond length depending on the degree of conjugation with the substituent. In all the cases the boron atom exhibited trigonal coordination with OH groups in *syn-anti* conformation. The conformation seems to be induced here by the relatively strong intramolecular O–H...N hydrogen bonds with estimated energy range of 6–10 kcal/mol. The molecular Hirshfeld surface analysis was used to show the probable active sites of the aromatic and aliphatic derivatives. The results revealed that the lack of aromatic or bulky substituent near N2 atom causes its activation as the effective H-bond acceptor. Otherwise the dimeric motif with boronic hydroxyl groups acting as donors and acceptors are found. The only exception is a 4-NO<sub>2</sub> phenyl substituted piperazine derivative where the long tail favors chain arrangement over the dimer. The phenyl rings of both the boronic and piperazine fragment take part in weak aromatic interactions, mostly of C–H...O and C–H... $\pi$  type. For aliphatic analogues the CH donors also come from piperazine ring. The investigated boronic acid analogue of MBZPZ drug (**5**) appeared to be the most effective dual molecule in terms of intermolecular interactions observed in crystal, hence, in our opinion, it is worth further biological evaluation tests.

## Experimental

<sup>1</sup>H and <sup>13</sup>C NMR spectra were recorded on Varian Mercury 400 or Varian Inova 500 spectrometers. The <sup>11</sup>B NMR spectra were recorded on Varian Unity Plus 200 operating at 64 MHz, chemical shifts were determined using inserts with BF<sub>3</sub>·Et<sub>2</sub>O in benzene ( $\delta = 0.0$  ppm). A drop of D<sub>2</sub>O has been added to the some of the samples to avoid additional signals corresponding to boroxines. Elemental analyses for C, H and N were obtained using Perkin Elmer CHNS/O II Model 240 analyser.

2-formylphenylboronic acid has been obtained by a standard procedure and its purity confirmed on the basis of <sup>1</sup>H NMR spectrum. All the starting piperazines have been purchased from Sigma-Aldrich and used without further purification.

**Synthesis of 2-((4-phenylpiperazin-1-yl)methyl)phenylboronic acid (1):** Solution of equimolar amounts of 2-formylphenylboronic (1 g, 6.6\*10<sup>-3</sup> mol) acid and *N*-phenylpiperazine (1.07g, 6.6\*10<sup>-3</sup> mol) in methanol (20 ml) was mixed at room temperature for 24 hours. NaBH<sub>4</sub> (1.96g, 6.6\*10<sup>-3</sup> mol) was added portion-wise to the resulting yellow solution while vigorous stirring. After 2 h of stirring white solid precipitated that was filtered off and recrystallized from a mixture of methylene chloride and acetonitrile (1.06 g, 54%), mp 257-259°C (from acetonitrile and methylene chloride mixture). Found: C, 68.7; H, 7.0; N, 9.3. Calc. for C<sub>17</sub>H<sub>21</sub>BN<sub>2</sub>O<sub>2</sub>: C, 68.8; H, 7.2; N, 9.5.  $\delta_{\text{H}}$ (400 MHz; (CD<sub>3</sub>)<sub>2</sub>SO) 2.55 (4H, s, br, 2xCH<sub>2</sub>), 3.11 (4H, s, br, 2xCH<sub>2</sub>), 3.61 (2H, s, CH<sub>2</sub>), 6.77 (1H, m, Ar), 6.90-6.92 (2H, m, Ar), 7.17-7.34 (5H, Ar), 7.66-7.67 (1H, m, Ar), 9.23 (2H, s, B(OH)<sub>2</sub>).  $\delta_{\text{C}}$ (100 MHz; (CD<sub>3</sub>)<sub>2</sub>SO) 47.9, 51.4, 62.9, 115.7, 119.2, 127.0, 129.1, 129.4, 130.2, 135.3, 141.3, 150.9.  $\delta_{\text{B}}$ (64.1 MHz; (CD<sub>3</sub>)<sub>2</sub>SO) 30. Crystals suitable for X-ray measurements have been obtained by crystallization from acetonitrile and methylene chloride mixture.

## Synthesis of 2, 5 and 6

Solutions of equimolar quantities of 2-formylphenylboronic acid and the corresponding piperazine in methanol was prepared at –10°C, followed by addition of NaBH<sub>4</sub> (1 eq.) and 20 min of subsequent vigorous stirring. Resulting mixtures were acidified with a 3 M HCl<sub>aq</sub>. The benzoxaborole side-product was removed by extraction with three portions of Et<sub>2</sub>O, according to the previously reported method.<sup>36</sup> The remaining aqueous phase has been neutralized with NH<sub>3</sub> aq (pH ca. 7). The desired boronic acids have been extracted with ethyl acetate. The organic phase was dried over anhydrous Na<sub>2</sub>SO<sub>4</sub> and evaporated under reduced pressure resulting in solid products.

**2-((4-(2-methoxyphenyl)piperazin-1-yl)methyl)phenylboronic acid (2):** (4.77 g, 57%), mp 163-165°C (from ethyl acetate). Found: C, 66.1; H, 6.9; N, 8.4. Calc. for C<sub>18</sub>H<sub>23</sub>BN<sub>2</sub>O<sub>3</sub>: C, 66.3; H, 7.0; N, 8.6.  $\delta_{\text{H}}$ (400 MHz; CDCl<sub>3</sub>) 2.74 (4H, s, br, 2xCH<sub>2</sub>), 3.14 (4H, s, br, 2xCH<sub>2</sub>), 3.71 (2H, s, CH<sub>2</sub>), 3.86 (3H, s, CH<sub>3</sub>), 6.85-7.02 (3H, m, Ar), 7.19-7.21 (1H, m, Ar), 7.32-7.37 (1H, m, Ar), 7.92-7.95 (2H, m, Ar), 8.57 (2H, s, br, B(OH)<sub>2</sub>).  $\delta_{\text{C}}$ (100 MHz; CDCl<sub>3</sub>) 50.0, 52.1, 55.2, 64.2, 111.1, 118.4, 120.9, 123.3, 127.5, 130.1, 130.5, 136.3, 140.6, 140.8, 152.0.  $\delta_{\text{B}}$ (64.1 MHz; (CD<sub>3</sub>)<sub>2</sub>CO) 33. Crystals suitable for X-ray measurements have been obtained by crystallization from acetonitrile.

**2-((4-methylpiperazin-1-yl)methyl)phenylboronic acid (5):** (0.36 g, 23%), mp 201-201°C (from ethyl acetate). Found: C, 61.7; H, 8.0; N, 11.9. Calc. for C<sub>12</sub>H<sub>19</sub>BN<sub>2</sub>O<sub>2</sub>: C, 61.6; H, 8.1; N, 11.9.  $\delta_{\text{H}}$ (400 MHz; (CD<sub>3</sub>)<sub>2</sub>CO+D<sub>2</sub>O) 2.17 (3H, s, Me), 2.47 (8H, s, br, 4 x CH<sub>2</sub>), 3.58 (2H, s, CH<sub>2</sub>), 7.19-7.22 (1H, m, Ar), 7.25-7.28 (1H, m, Ar), 7.29-7.34 (1H, m, Ar).  $\delta_{\text{C}}$ (100 MHz; (CD<sub>3</sub>)<sub>2</sub>CO+D<sub>2</sub>O) 45.8, 52.4, 55.2, 64.42, 127.8, 130.4, 131.4, 136.9, 142.1, 163.8.  $\delta_{\text{B}}$ (64.1 MHz; (CD<sub>3</sub>)<sub>2</sub>CO+D<sub>2</sub>O) 29.8, 20.5. Crystals suitable for X-ray measurements have been obtained by crystallization from acetonitrile.

**2-((4-benzhydrylpiperazin-1-yl)methyl)phenylboronic acid (6):** (2.06 g, 80%), mp 182-184°C, partial melting at 98 and 158°C (from acetone). Found: C, 72.9; H, 7.5; N, 6.2. Calc. for C<sub>24</sub>H<sub>27</sub>BN<sub>2</sub>O<sub>2</sub>\* (CH<sub>3</sub>)<sub>2</sub>CO: C, 72.9; H, 7.5; N, 6.4.  $\delta_{\text{H}}$ (400 MHz; (CD<sub>3</sub>)<sub>2</sub>CO + drop of D<sub>2</sub>O) 2.51 (8H, s, br, 4xCH<sub>2</sub>), 3.61 (2H, s, CH<sub>2</sub>), 4.28 (1H, s, CH), 7.12-7.18 (2H, m, Ar), 7.19-7.31 (7H, m, Ar), 7.43-7.47 (2H, m, Ar), 7.83-7.85 (1H, m, Ar), 9.15 (2H, s, B(OH)<sub>2</sub>, minor intensity).  $\delta_{\text{C}}$ (100 MHz; (CD<sub>3</sub>)<sub>2</sub>CO + drop of D<sub>2</sub>O) 51.1, 51.8, 63.5, 75.5, 126.8, 126.7, 127.6, 128.4, 129.5, 130.5, 136.0, 141.3, 142.9.  $\delta_{\text{B}}$ (64.1 MHz; (CD<sub>3</sub>)<sub>2</sub>CO + drop of D<sub>2</sub>O) 30. Crystals suitable for X-ray measurements have been obtained by crystallization from acetone and contained acetone molecule within the crystal.

**2-((4-(2,3-dichlorophenyl)piperazin-1-yl)methyl)phenylboronic acid (3):** Solution of equimolar quantities of 2-formylphenylboronic acid and 2,3-dichlorophenylpiperazine in 50 ml of methanol was prepared at –12°C, followed by addition of NaBH<sub>4</sub> (1 eq.) and 20 min of subsequent vigorous stirring. 3 M HCl<sub>aq</sub> was added till pH of the mixture was ~ 1 following with 10 min of stirring. The post-reaction mixture was extracted with Et<sub>2</sub>O (1x60 ml, 2x30 ml). The remaining aqueous phase has been neutralized with NH<sub>3</sub> aq (pH ca. 7). The desired boronic acid has been extracted with Et<sub>2</sub>O (3x30 ml). The organic phase was dried over anhydrous Na<sub>2</sub>SO<sub>4</sub> and evaporated under reduced pressure resulting in solid product (yield 22%). The crude product was washed with acetone resulting in pure 3. Crystals suitable for X-ray measurements have been obtained by crystallization from acetone.  $\delta_{\text{H}}$ (500 MHz; DMSO) 2.60 (4H, s, br, 2xCH<sub>2</sub>), 2.99 (4H, s, br, 2xCH<sub>2</sub>), 3.65 (2H, s, CH<sub>2</sub>), 7.13-7.34 (6H, m, Ar), 7.68-7.70 (1H, m, Ar), 9.14 (2H, s, B(OH)<sub>2</sub>).  $\delta_{\text{C}}$ (126 MHz, DMSO) 150.8, 141.0, 135.2, 132.5, 130.1, 129.2, 128.5, 126.7, 126.0, 124.4, 119.6, 62.8, 51.5, 50.3.  $\delta_{\text{B}}$ (CD<sub>3</sub>OD) 14.

**2-((4-(4-nitrophenyl)piperazin-1-yl)methyl)phenylboronic acid (4):** Solution of 2-formylphenylboronic acid (2 eq.) and p-nitrophenylpiperazine (1 eq.) in methanol (45 ml) was prepared at  $-10^{\circ}\text{C}$ , followed by addition of  $\text{NaBH}_4$  (1 eq.) and 20 min of subsequent vigorous stirring.  $3\text{M HCl}_{\text{aq}}$  (15 ml) was added and mixture was stirred for another 10 min., followed by extraction with  $\text{Et}_2\text{O}$  (1x30 ml, 2x40ml). The remaining aqueous phase has been neutralized with  $\text{NH}_3_{\text{aq}}$  (pH ca. 7). The desired boronic acid has been extracted with  $\text{Et}_2\text{O}$  (3x30 ml). The organic phase was dried over anhydrous  $\text{Na}_2\text{SO}_4$  and evaporated under reduced pressure resulting in solid product (yield 10%).  $\delta_{\text{H}}$  (500 MHz;  $(\text{CD}_3)_2\text{CO}$  + drop of  $\text{D}_2\text{O}$ ) 2.64 (4H, s, br,  $2\times\text{CH}_2$ ), 3.50 (4H, s, br,  $2\times\text{CH}_2$ ), 3.67 (2H, s,  $\text{CH}_2$ ), 7.01-7.03 (2H, m, Ar), 7.20-7.22 (1H, m, Ar), 7.26-7.33 (2H, m, Ar), 7.76-7.78 (1H, m, Ar), 8.03-8.05 (2H, m, Ar).  $\delta_{\text{C}}$  ( $(\text{CD}_3)_2\text{CO}$  + drop of  $\text{D}_2\text{O}$ ) 46.7, 51.7, 63.5, 113.7, 126.3, 127.9, 130.4, 130.9, 136.2, 138.5, 141.5, 155.6.  $\delta_{\text{B}}$  ( $(\text{CD}_3)_2\text{CO}$  + drop of  $\text{D}_2\text{O}$ ): 32, 23

**X-ray diffraction:** The single crystal X-ray experiments were conducted on the Gemini A Ultra Diffractometer (Agilent Technologies). Data collection and data reduction were performed in the CrysAlis<sup>Pro</sup> program.<sup>45</sup> To solve and refine the structures OLEX-2 suite<sup>46</sup> with implemented SHELX program<sup>47</sup> was used. Further details of structural studies are given in Supplementary Information. The crystallographic data are summarized in Table 2. CCDC 1040156-1040161 contain the supplementary crystallographic data for this paper. These data can be obtained free of charge from The Cambridge Crystallographic Data Centre via [www.ccdc.cam.ac.uk/data\\_request/cif](http://www.ccdc.cam.ac.uk/data_request/cif).

**Calculations:** Estimation of O–H...O hydrogen bonds energy was based on the Lippincott and Schroeder one dimensional H-bond model.<sup>29</sup> It is a semi-empirical method for calculating binding energies of the H-bond starting from its geometry. Therefore, the O–H bond lengths were normalized to be consistent with these obtained from neutron diffraction studies and are equal to 0.93 Å.<sup>48</sup> The algorithm and parameterization was implemented in the LSHB program available as a courtesy by Professors Paola and Gastone Gilli.<sup>49</sup>

The molecular Hirshfeld surfaces (HS)<sup>28</sup> were generated using Crystal Explorer 3.1 program.<sup>50</sup> They are constructed basing on the electron distribution calculated as the sum of spherical atom electron densities. The HS enclosing a molecule is defined by points where the contribution to the electron density from the molecule of interest is equal to the contribution from all the other molecules. For each point on that isosurface two distances are defined:  $d_e$ , the distance from the point to the nearest nucleus external to the surface, and  $d_i$  the distance to the nearest nucleus internal to the surface. The presented in Figure 4 surfaces are in form of maps showing  $d_i$  and  $d_e$  distances, respectively. The red-yellow-green colouring scheme represents short to long distances.

## Acknowledgements

Financial support by the Ministry of Science and Higher Education (Grant NN204 135639) is kindly acknowledged. K.C. acknowledges the support of the Faculty of Chemistry, Warsaw University of Technology. This work has been supported by the European Union in the framework of European Social Fund through the Warsaw University of Technology Development Program by the scholarship awarded by the Center of Advanced Studies for Alicja Matuszewska.

## Notes and references

<sup>a\*</sup> Faculty of Chemistry, Warsaw University of Technology  
00-664 Warsaw, Noakowskiego 3, Poland  
E-mail: [agnieszka@ch.pw.edu.pl](mailto:agnieszka@ch.pw.edu.pl)

Electronic Supplementary Information (ESI) available: details on X-ray diffraction studies, selected geometrical parameters for studied compounds, parameters of weak intermolecular interactions, packing diagrams. See DOI: 10.1039/b000000x/

- 1 a) J. B. Bremner, B. Coban, R. Griffith, K. M. Groenewoud and B. F. Yates, *Bioorg. Med. Chem.* 2000, **8**, 201; b) L. Santana, E. Uriarte, Y. Fall, M. Teixeira, C. Terán, E. García-Martínez and B. Tolf, *Eur. J. Med. Chem.* 2002, **37**, 503; c) Pontillo, J. A. Tran, B. A. Fleck, D. Marinkovic, M. Arellano, F. C. Tucci, M. Lanier, J. Nelson, J. Parker, J. Saunders, B. Murphy, A. C. Foster and C. Chen, *Bioorg. Med. Chem. Lett.* 2004, **14**, 5605; d) T. Takahashi, A. Sakuraba, T. Hirohashi, T. Shibata, M. Hirose, Y. Haga, K. Nonoshita, T. Kanno, J. Ito, H. Iwaasa, A. Kanatani, T. Fukami and N. Sato, *Bioorg. Med. Chem.* 2006, **14**, 7501; e) M. Tomić, D. Ignjatović, G. Tovilović, D. Andrić, G. Roglić and S. Kostić-Rajačić, *Bioorg. Med. Chem. Lett.* 2007, **17**, 5749.
- 2 J. Handzlik, H. H. Pertz, T. Görnemann, S. Jähnichen and K. Kieć-Kononowicz, *Bioorg. Med. Chem. Lett.* 2010, **20**, 6152.
- 3 a) P. Chaudhary, R. Kumar, A. K. Verma, D. Singh, V. Yadav, A. K. Chhillar, G. L. Sharmab and R. Chandra, *Bioorg. Med. Chem.* 2006, **14**, 1819; b) J. Jin, X. Wang and L. Kong, *Bioorg. Med. Chem. Lett.* 2011, **21**, 909; c) V. Canale, P. Guzik, R. Kurczab, P. Verdie, G. Satała, B. Kubica, M. Pawłowski, J. Martinez, G. Subra, A. J. Bojarski and P. Zajdel, *Eur. J. Med. Chem.* 2014, **78**, 10.
- 4 a) N. Güler, B. Eryonucu, A. Güneş, Ü. Güntekin, M. Tuncer and H. Özbek, *Cardiovasc. Drug Ther.* 2003, **17**, 371; b) A. Abdelbary, O. N. El-Gazayerly, N. A. El-Gendy and A. A. Ali, *AAPS PharmSciTech.* 2010, **11**, 1058 and references cited.
- 5 a) S. Rotzinger, M. Bourin, Y. Akimoto, R. T. Coutts and G. B. Baker, *Cell. Mol. Neurobiol.* 1999, **19**, 427-442 and references cited; b) P. Gareri, U. Falconi, P. De Fazio and G. De Sarro, *Prog. Neurobiol.* 2000, **61**, 353 and references cited.
- 6 S. M. Herman, R. B. Vender and J. Cutan. *Med. Surg.* 2003, **7**, 467 and references cited.
- 7 F. A. Siddiqui, A. Z. Mirza, M. H. Zuberi and F. Qureshi, *Med. Chem. Res.* 2011, **20**, 121 and references cited.
- 8 S. Shi, H. Chen, X. Lin and X. Tang, *Int. J. Pharm.* 2010, **383**, 264.
- 9 a) H. J. Möller, *Eur. Arch. Psychiatry Clin. Neurosci.* 2005, **255**, 190 and references cited; b) M. Kuloglu, O. Ekinci, Y. Albayrak and A. Caykoylu, *Arch. Women Ment. Health* 2010, **13**, 443 and references cited.
- 10 E. Lacivita, M. Leopoldo, P. De Giorgio, F. Berardi and R. Perrone, *Bioorg. Med. Chem.* 2009, **17**, 1339.
- 11 a) J. C. Lin, N. Bangs, H. Lee, R. R. Kydd and B. R. Russell, *Psychopharmacology* 2009, **207**, 439; b) B. M. Z. Cohen, R. Butler, *Int. J. Drug Policy* 2011, **22**, 95.
- 12 a) D. de Boer, I. J. Bosman, E. Hidvégi, C. Manzoni, A. A. Benkő, L. J. A. L. dos Reys and R. A. A. Maes, *Forensic Sci. Int.* 2001, **121**, 47; b) R. F. Staack, L. D. Paul, D. Schmid, G. Roider and B. Rolf, *J. Chromatogr. B* 2007, **855**, 127; d) R. F. Staack, *Lancet* 2007, **369**, 1411.
- 13 a) M. Mohty, D. Blaise, D. Olive and B. Gaugler, *Trends Mol. Med.* 2005, **11**, 397; b) T. Tauchi and K. Ohyashiki, *Int. J. Hematol.* 2006, **83**, 294.
- 14 L. R. Dick and P. E. Fleming, *Drug Discov. Today* 2010, **15**, 243.
- 15 D. G. Hall in *Boronic Acids. Preparation and Applications in Organic Synthesis, Medicine and Materials*. Second, Completely Revised Edition; (Ed. D. G. Hall), Wiley-VCH, Weinheim, 2011.

- 16 R. Smoum, A. Rubinstein, V. M. Dembitsky and M. Srebnik, *Chem. Rev.* 2012, **112**, 4156.
- 17 L. Zhu, S. H. Shabbir, M. Gray, V. M. Lynch, S. Sorey and E. V. Anslyn, *J. Am. Chem. Soc.* 2006, **128**, 1222.
- 18 T. D. James, M. D. Phillips and S. Shinkai, *Boronic Acids in Saccharide Recognition* (RSC Publishing, Cambridge, 2006).
- 19 V. J. Stella and K. W. Nti-Addae, *Adv. Drug Deliv. Rev.* 2007, **59**, 677.
- 20 J. Spencer, C. B. Baltus, N. J. Press, R. W. Harrington and W. Clegg, *Tetrahedron Lett.* 2011, **52**, 3963.
- 21 J. Jin, B. Budzik, Y. Wang, D. Shi, F. Wang, H. Xie, Z. Wan, C. Zhu, J. J. Foley, E. F. Webb, M. Berlanga, M. Burman, H. M. Sarau, D. M. Morrow, M. L. Moore, R. A. Rivero, M. Palovich, M. Salmon, K. E. Belmonte and D. I. Lainé, *J. Med. Chem.* 2008, **51**, 5915.
- 22 C. Chen, P. Dagneau, E. J. J. Grabowski, R. Oballa, P. O'Shea, P. Prasit, J. Robichaud, R. Tillyer and X. Wang, *J. Org. Chem.* 2003, **68**, 2633.
- 23 a) A. M. Davis, S. J. Teague and G. J. Kleywegt, *Angew. Chem. Int. Ed.* 2003, **42**, 2718; b) F. H. Allen and R. Taylor, *Chem. Commun.* 2005, 5135; c) R. Taylor, J. Cole, O. Korb and P. McCabe, *J. Chem. Inf. Model.* 2014, **54**, 2500.
- 24 T. G. Davies and M. Hyvönen (Eds) *Fragment-Based Drug Discovery and X-Ray Crystallography*, Springer Science & Business Media, 2012.
- 25 K. A. Brameld, B. Kuhn, D. C. Reuter and M. Stahl, *J. Chem. Inf. Model.* 2008, **48**, 1.
- 26 M. L. Verdonk, J. C. Cole, P. Watson, V. Gillet and P. Willett, *J. Mol. Biol.* 2001, **307**, 841.
- 27 J. W. M. Nissink and R. Taylor, *Org. Biomol. Chem.* 2004, **2**, 3238.
- 28 a) J. J. McKinnon, M. A. Spackman and A. S. Mitchell, *Acta Crystallogr. B* 2004, **60**, 627; b) M. A. Spackman and D. Jayatilaka, *CrystEngComm.* 2009, **11**, 19.
- 29 a) E. R. Lippincott and R. Schroeder *J. Chem. Phys.* 1955, **23**, 1099; b) R. Schroeder and E. R. Lippincott, *J. Phys. Chem.* 1957, **61**, 921.
- 30 a) J. Spencer, A. P. Burd, C. A. Goodwin, S. A. M. Mérette, M. F. Scully, T. Adatia and J. J. Deadman, *Tetrahedron* 2002, **58**, 1551; b) J. Spencer, C. B. Baltus, H. Patel, N. J. Press, S. K. Callear, L. Male and S. J. Coles, *ACS Comb. Sci.* 2011, **13**, 24.
- 31 A. Adamczyk-Woźniak, K. M. Borys, I. D. Madura, S. Michałek and A. Pawełko, *Tetrahedron* 2013, **69**, 8936.
- 32 I. D. Madura, K. Czerwińska, M. Jakubczyk, A. Pawełko, A. Adamczyk-Woźniak and A. Sporzyński, *Cryst. Growth Des.* 2013, **13**, 5344.
- 33 A. Adamczyk-Woźniak, M. K. Cyrański, B. T. Frączak, A. Lewandowska, I. D. Madura and A. Sporzyński, *Tetrahedron* 2012, **68**, 3761.
- 34 a) T. Holyoak, M. A. Wilson, T. D. Fenn, C. A. Kettner, G. A. Petsko, R. S. Fuller and D. Ringe, *Biochemistry* 2003, **42**, 6709; b) T. I. Lazarova, L. Jin, M. Rynkiewicz, J. C. Gorga, F. Bibbins, H. V. Meyers, R. Babineb and J. Strickler, *Bioorg. Med. Chem. Lett.* 2006, **16**, 5022.
- 35 a) P. Chaudhary, S. Nimesh, V. Yadav, A. Kr. Verma and R. Kumar, *Eur. J. Med. Chem.* 2007, **42**, 471; b) J. P. Safko and R. D. Pike, *J. Chem. Crystallogr.* 2012, **42**, 981.
- 36 A. Adamczyk-Woźniak, I. Madura, A. Pawełko, A. Sporzyński, A. Żubrowska and J. Żyła, *Cent. Eur. J. Chem.* 2011, **9**, 199.
- 37 L. J. Farrugia, *J. Appl. Crystallogr.* 1997, **30**, 565.
- 38 a) I. D. Madura, K. Czerwińska and D. Soldańska, *Cryst. Growth Des.* 2014, **14**, 5912; b) I. D. Madura, A. Adamczyk-Woźniak and A. Sporzyński, *J. Mol. Struct.* 2015, **1083**, 204.
- 39 A. Adamczyk-Woźniak, Z. Brzózka, M. Dąbrowski, I. D. Madura, R. Scheidsbach, E. Tomecka, K. Żukowski and A. Sporzyński, *J. Mol. Struct.* 2013, **1035**, 190.
- 40 M. C. Etter, J. C. MacDonald and J. Bernstein, *Acta Crystallogr. B* 1990, **46**, 256.
- 41 P. Gilli, L. Pretto, V. Bertolasi and G. Gilli, *Acc. Chem. Res.* 2009, **42**, 33.
- 42 A. Adamczyk-Woźniak, K. M. Borys, I. D. Madura, A. Pawełko, E. Tomecka and K. Żukowski, *New J. Chem.* 2013, **37**, 188.
- 43 H. Pessoa-Mahana, G. Recabarren-Gajardo, J. Fiedler Temer, G. Zapata-Torres, C. D. Pessoa-Mahana, C. Saitz Barriá and R. Araya-Maturana *Molecules* 2012, **17**, 1388.
- 44 A. I. Kitajgorodskij, *Molecular Crystals and Molecules*, New-York Academic Press, 1973.
- 45 CrysAlisPro, Agilent Technologies, Version 1.171.36.21 (release 14 - 08-2012 CrysAlis171 .NET).
- 46 O. V. Dolomanov, L. J. Bourhis, R. J. Gildea, J. A. K. Howard and H. J. Puschmann, *J. Appl. Crystallogr.* 2009, **42**, 339.
- 47 G. M. Sheldrick, *Acta Crystallogr. A* 2008, **64**, 112.
- 48 F. H. Allen, *Acta Crystallogr. B* 1986, **42**, 515.
- 49 P. Gilli and G. Gilli, LSHB. A Computer program for performing Lippincott and Schroeder HB calculations Department of Chemistry, University of Ferrara, Ferrara, Italy, 1992.
- 50 CrystalExplorer (Version 3.1) S. K. Wolff, D. J. Grimwood, J. J. McKinnon, M. J. Turner, D. Jayatilaka, M. A. Spackman, University of Western Australia, 2012.

## ARTICLE

**Table 2.** Crystallographic data collection and refinement parameters for 1-6.

Compound	1	2	3	4	5	6
Empirical formula	C <sub>17</sub> H <sub>21</sub> BN <sub>2</sub> O <sub>2</sub>	C <sub>18</sub> H <sub>23</sub> BN <sub>2</sub> O <sub>3</sub>	C <sub>17</sub> H <sub>19</sub> BClN <sub>2</sub> O <sub>2</sub>	C <sub>17</sub> H <sub>20</sub> BN <sub>3</sub> O <sub>4</sub>	C <sub>12</sub> H <sub>19</sub> BN <sub>2</sub> O <sub>2</sub> , H <sub>2</sub> O	C <sub>24</sub> H <sub>27</sub> BN <sub>2</sub> O <sub>2</sub> , C <sub>3</sub> H <sub>6</sub> O
M <sub>w</sub> [g·mol <sup>-1</sup> ]	296.17	326.19	365.05	341.17	252.12	444.36
crystal size [mm]	0.40×0.60×0.60	0.08×0.24×0.48	0.16×0.21×0.25	0.20×0.50×0.60	0.40×0.50×0.60	0.40×0.45×0.50
T [K]	100(2)	100(2)	120(2)	100(2)	100(2)	100(2)
Radiation	Mo-K $\alpha$	Cu-K $\alpha$	Cu-K $\alpha$	Cu-K $\alpha$	Cu-K $\alpha$	Cu-K $\alpha$
Wave length [Å]	0.7107	1.5418	1.5418	1.5418	1.5418	1.5418
Crystal system	monoclinic	monoclinic	triclinic	monoclinic	orthorhombic	monoclinic
Space group	<i>P</i> 2 <sub>1</sub> / <i>c</i>	<i>I</i> 2/ <i>a</i>	<i>P</i> -1	<i>P</i> 2 <sub>1</sub> / <i>n</i>	<i>Pna</i> 2 <sub>1</sub>	<i>P</i> 2 <sub>1</sub> / <i>c</i>
<i>a</i> [Å]	13.3088(2)	12.1978(3)	7.9155(4)	10.32568(6)	12.87751(17)	24.60371(16)
<i>b</i> [Å]	6.01200(10)	19.2053(5)	10.3130(4)	9.10656(10)	10.18562(12)	11.76829(7)
<i>c</i> [Å]	19.8330(2)	15.5424(4)	11.8333(7)	18.03844(12)	10.36536(14)	17.52165(11)
$\alpha$ [°]	90	90	88.456(4)	90	90	90
$\beta$ [°]	108.6467(14)	96.000(3)	72.897(5)	90.7068(6)	90	93.8287(6)
$\gamma$ [°]	90	90	69.370(4)	90	90	90
<i>V</i> [Å <sup>3</sup> ]	1503.59(4)	3621.05(16)	860.88(8)	1696.05(2)	1359.58(3)	5061.96(6)
<i>Z</i>	4	8	2	4	4	8
$\rho_{\text{calcd}}$ [Mg m <sup>-3</sup> ]	1.308	1.197	1.408	1.336	1.232	1.166
$\mu$ [mm <sup>-1</sup> ]	0.085	0.648	3.489	0.782	0.704	0.592
<i>T</i> <sub>min</sub> , <i>T</i> <sub>max</sub>	0.838, 1.000	0.736, 1.000	0.485, 1.000	0.439, 1.000	0.704, 1.000	0.801, 1.000
<i>F</i> (000)	632	1392	380	720	544	1904
Reflections collected	32627	13981	7576	77017	10784	161927
Independent reflection [ <i>R</i> <sub>int</sub> ]	3282 [2.47%]	3226 [3.11%]	3018 [4.14%]	3017 [6.7%]	2186 [2.54%]	8915 [4.07%]
Reflections with <i>I</i> > 2 $\sigma$ ( <i>I</i> )	3053	2777	2863	2922	2143	8238
$\theta_{\text{min}} - \theta_{\text{max}}$	3.23 - 27.00	3.67 - 67.09	3.92 - 66.49	4.90 - 67.07	5.54 - 67.21	3.36 - 66.50
GOF on <i>F</i> <sup>2</sup>	1.043	1.058	1.034	1.062	1.089	1.027
$\Delta\rho_{\text{min}/\text{max}}$ [e Å <sup>-3</sup> ]	-0.209 / 0.418	-0.169 / 0.256	-0.685 / 0.427	-0.193 / 0.253	-0.453 / 0.211	-0.298 / 0.429
Final <i>R</i> indices ( <i>I</i> > 2 $\sigma$ ( <i>I</i> ))	<i>R</i> <sub>1</sub> = 0.0345 <i>wR</i> <sub>2</sub> = 0.0919	<i>R</i> <sub>1</sub> = 0.0392 <i>wR</i> <sub>2</sub> = 0.1020	<i>R</i> <sub>1</sub> = 0.0478 <i>wR</i> <sub>2</sub> = 0.1262	<i>R</i> <sub>1</sub> = 0.0364 <i>wR</i> <sub>2</sub> = 0.0976	<i>R</i> <sub>1</sub> = 0.0373 <i>wR</i> <sub>2</sub> = 0.1052	<i>R</i> <sub>1</sub> = 0.0357 <i>wR</i> <sub>2</sub> = 0.0883
<i>R</i> indices (all data)	<i>R</i> <sub>1</sub> = 0.0365 <i>wR</i> <sub>2</sub> = 0.0931	<i>R</i> <sub>1</sub> = 0.0458 <i>wR</i> <sub>2</sub> = 0.1059	<i>R</i> <sub>1</sub> = 0.0493 <i>wR</i> <sub>2</sub> = 0.1288	<i>R</i> <sub>1</sub> = 0.0372 <i>wR</i> <sub>2</sub> = 0.0984	<i>R</i> <sub>1</sub> = 0.0381 <i>wR</i> <sub>2</sub> = 0.1064	<i>R</i> <sub>1</sub> = 0.0385 <i>wR</i> <sub>2</sub> = 0.0905